The influence of time horizon on energy hub sizing

François Lédée[1,2], Curran Crawford[1,3], Ralph Evins[1,2]
[1]Institute for Integrated Energy Systems, University of Victoria, British Columbia, Canada
[2]Energy in Cities group, Department of Civil Engineering, University of Victoria, British Columbia, Canada
[3]Sustainable Systems Design Lab, Department of Mechanical Engineering, University of Victoria, British Columbia, Canada

Abstract

Sizing energy hubs with interdependent loads, energy sources and devices is a computationally intensive task requiring at least a year of hourly data per load and source. Methods (e.g. using key-days) address this shortage, however none of these attempt to identify the important statistical features in the time series influencing the system sizing.

This study investigates the influence of using shorter time horizons on energy hub sizing for single buildings, and tries to identify critical periods or time steps.

We find the operational control trajectory of a building energy system is not influenced by the horizon, while the sizing is. Storage technologies play a dominant role in the results, and are extensively used, while the storage sizing results from a complex interplay between charging/discharging speed, storage capacity and use of other technologies in the system.

Introduction

Integration of renewable energy to reduce the carbon footprint of building energy loads requires a careful sizing from the earliest design stages. To this end, system modeling using linear programming is gaining interests among practitioners (Hoffmann et al. (2020); Teichgraeber and Brandt (2022)). However these methods are slow as they require a solution over at least a full year of time series data.

To reduce the computation burden, exploiting the quasi-redundancy of building energy demands and solar irradiation (Hoffmann et al. (2020); Bahl et al. (2018)) allows the usage of a reduced number of pieces of information, from months to days. Using representative days selected via clustering algorithms has now become common practice (Kotzur et al. (2018)).

The selection process for these representative periods is usually based on time series information, i.e. independently from the system itself. Some iterative frameworks were suggested to reduce this shortcoming (Fitiwi et al. (2015); Bahl et al. (2018)), e.g. to include extreme periods (Teichgraeber et al. (2020)).

Though the results of all suggested methods are considered as is and the importance of each piece of information remains unknown (Hoffmann et al. (2020)).

This study performs and analyses system sizing and operation results for different time series horizons (day to 3 months). Questions driving this study are:

- What influence does the time series horizon have on the sizing and operation of an energy system?
- Does the sizing with a reduced horizon allow identification of decisive periods or time steps?
- What are the consequences on computation time?

A methodology section introduces the framework, hypotheses and study cases. Then results are exposed and discussed. The conclusion summarizes our findings.

Methodology

Energy Hub modeling

In this work, the energy systems are modeled as energy hubs. An energy hub (EH) is an interface between various facilities, sources and loads. It represents a framework to model the management (conversion, conditioning, storage) of multiple energy carriers (Geidl et al. (2007)). This approach considers the interaction between elements of the energy system during the sizing procedure.

Mixed-integer linear programming (MILP) is used to represent and size the energy system. The objective function to minimize and governing set of equations are described by Evins et al. (2014). A key equation when considering different time horizons is the storage looping constraint (eq.1), forcing the storage state of charge (SOC) to be identical at the start ($t = 0$) and end ($t = T + 1$) of a period.

$$SOC(T+1) = SOC(0) \tag{1}$$

We also highlight the capacity related constraints, further analysed in this study. The energy output ($p_{out,c}$) of a converter c can not exceed the devices capacity P_c (eq.2). Similarly the SOC of a storage device s does not exceed its capacity P_s (eq.3). A storage ramping constraint limits the energy in/outflow $Q_{s,+/-}$ to a fraction λ of the capacity (eq.4).

$$0 \leq p_{out,c}(t) \leq P_c \ \forall c, t \tag{2}$$

$$0 \leq SOC_s(t) \leq P_s \ \forall s, t \tag{3}$$

$$0 \leq Q_{s,+/-}(t) \leq \lambda \times P_s \ \forall s, t \tag{4}$$

The total carbon emissions is also computed using carbon emission factors of grid electricity and gas. The ϵ-constraint (Murray et al. (2020)) is used on the carbon emissions during the sizing step to explore optimal solutions at minimum cost, -50% CO_2 emissions and net-zero (NZ). Note that -50% CO_2 emission scenarios force CO_2 emissions to be *at least* reduced by 50% relatively to the minimum cost solution, though optimal solutions may result in even lower CO_2 emission levels.

The experiment

The experiment compares the sizing and operation of an EH for different time horizons: day, week, month, quarter. All are viewed as *estimates* and compared to the optimization using a year of data, considered as ground *truth*.

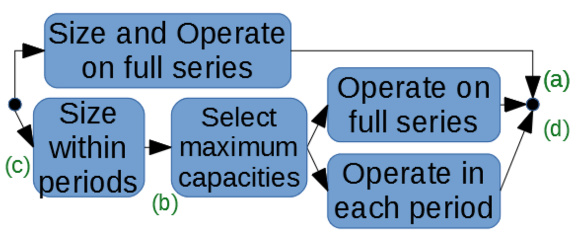

Figure 1: Methodology

The experiment consists of 3 steps: a sizing step in each period, the selection of capacities from these periods, and an operation step (Figure 1). For each horizon length, the timeline is subdivided in periods of one horizon. During the sizing step, optimal device capacities and operations are computed independently over each period. The resulting CO_2 emissions at minimum cost in each period are used to set the emission threshold of the -50% CO_2 scenarios. During the operation step, the highest capacities obtained over all periods (of equal length horizon) are then used and the resulting energy system is operated, both for one year of hourly data and independently in each shorter period length, estimating the cost and carbon emissions again. The operation in each period uses the same CO_2 emission threshold as during the sizing, while operations on the full time series use the sum of CO_2 emission obtained after sizing of all periods. In every case, the total cost is minimized.

The study first compares overall results (a). The sizing results from each periods is further analysed to capture the decisive periods (b). To identify critical elements for the sizing, we localize the time steps at which equations (2-4) are binding (c). Finally, computation times are also compared (d).

Case Study

The study is conducted for 5 locations in different climate zones (Duluth MN, Seattle WA, Baltimore MD, Los Angeles CA, Houston TX), using data from Hourly Load Profiles of Commercial and Residential Buildings dataset[1] (Wilson (2014)). In each location, 2 building types are considered (residential and small-office) across 4 scenarios (Table 1). Other modeling parameters were based on energy hub studies and manufacturers data. All codes and data are made available on a git repository[2].

The energy system to be sized is shown in Figure 2, and includes photovoltaic (PV) panels, a heat-pump (HP), Boiler, a hot water tank (HWT) and a battery. The PV efficiency is precomputed using the Python package Gsee[3] (Pfenninger and Staffell (2016)). The EH framework uses the Besos[4] (Westermann et al. (2021)) package and the Gurobi solver (Gurobi Optimization (2021)).

Table 1: Price scenarios used.

#	Price ($\frac{\$}{kWh}$)			Carbon ($\frac{gCO_{2,eq}}{kWh}$)	
	Electricity	Gas	Feed-in	Electricity	Gas
1	0.1	0.02	0.05	200	400
2	0.33	0.02	0.05	600	400
3	0.1	0.1	0.05	200	400
4	0.33	0.1	0.05	600	400

Results

Influence of horizons on the estimations

Figure 3 shows the optimal capacity-carbon fronts obtained after the sizing and operation steps in Seattle and Houston. Capacities are determined after the sizing step, CO_2 emission levels are obtained after operating the so sized system on one entire year.

The obtained fronts are similar in shape for every time

[1] https://data.openei.org/submissions/153
[2] https://gitlab.com/fledee/horizon_ehub
[3] https://pypi.org/project/gsee/
[4] https://pypi.org/project/besos/

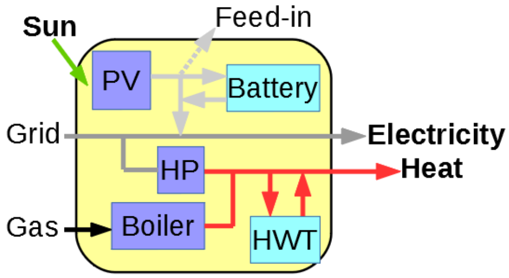

Figure 2: System design

horizon, except for the HWT (Figures 3d & 3h) and HP in Seattle (Figure 3a). PV and Battery show an exponential capacity increase with decreasing CO_2 limits for all horizons. This reveals that the importance of both technologies and their interplay can be correctly captured in specific shorter time spans. The HWT is usually only installed at net-zero and for horizons of a month or less. HP capacity profiles show a binary decision to either fully electrify the heating demand (-50% CO_2 and NZ) or discard the technology (minimum cost). At -50% CO_2 in Seattle (Figure 3a) the reference show an intermediate HP capacity, this reveals that considering an entire year of data incentivizes a joint use of HP and Boiler. The presence of HWT at NZ also matches with a reduced need of HP capacity (Figure 3e for days to months) or an increased need (Figure 3a), as developed in the 3^{rd} results subsection.

Profiles may also differ in CO_2 emission levels. For the -50% CO_2 emissions scenarios, the shorter the horizon for the sizing, the lower the emissions. At minimum cost, shorter horizons increase the CO_2 emissions. Sizing in Houston (Figures 3e-3h) illustrates that shorter time horizons result in energy systems with higher PV and Battery capacities than the yearly reference. Optimal operation of these systems result in significantly lower CO_2 emissions than the reference case.

Figure 4 explains this phenomenon: the expected CO_2 emissions right after the sizing step are systematically higher with sub-yearly horizons than with the yearly reference. Conversely after operating so sized systems, the emission level become smaller than the reference. The shorter the horizon, the greater the reduction. Using shorter time horizons results either in a larger electrification of the heating demand (Figure 3a) or a higher use of PV and battery (Figures 3f, 3g & 5) to meet the carbon reduction constrain in periods with less resources. These greater capacities become available for all periods during the operation step, and their usage results in CO_2 emissions lower than the reference case. This is highlighted in Figure 5, where a storage is only installed for a few independent days but used extensively during the operating phase.

The horizon of the operation step does not influence our results, regardless of the location, scenario or building type. Figure 5 shows a battery system operated with a year and a day of horizon, where the same daily cycles are observed. The strong daily cycles and low variability of profiles induced by simulated single building archetypes can explain this observation, as well as the use of constant energy prices.

Informative value of sizing results

Figure 6 illustrates the diversity of sizing results obtained throughout all study cases, with a $\pm 5\%$ margin regarding the results from the full optimization. A margin of 5% is chosen, similarly to the optimality gap in the optimization problem. Some cases allow a clear identification of decisive periods, narrowing down the scope as shorter horizons are considered (e.g. NZ in Figure 6). Other show systematic divergences with the full optimization (e.g. min. cost and -50% CO_2 in Figure 6c) or a mix of periods leading to accurate sizing, oversizing and undersizing (e.g. Figures 6a-6b at -50% CO_2).

Regardless of the horizon and carbon scenario, the optimization in most periods lead to a capacity underestimation (Figure 6). Notice that some periods of shorter horizon do yield accurate results. There generally exists periods for which the Heat-Pump is accurately sized, regardless of the horizon, location or constraint on carbon reduction (Figure 6a). We also find cases where using a year horizon systematically leads to different sizings (Figure 6c at -50% CO_2), or where shorter horizons lead to using a technology that otherwise wouldn't have been recommended (Figure 6c at min. cost).

The existence of at least one of these periods is not guaranteed, while being more likely with shorter horizons (Table 2). Highest probabilities in all locations are found with the heat-pump sizing. The existence of such periods is also likely for PV and Battery at NZ, when the system mostly rely on them. With a carbon reduction constraint, the likelihood that periods yield a sizing similar to the yearly horizon one increases with shorter periods. At min. cost, the horizon has little effect on the sizing, as the system rely on grid and gas imports in most cases.

Decisive elements

Figure 7 shows an example of a heat-pump usage *during the sizing step* and the moments when the devices operate at their maximum, i.e when the capacity constraint (2) is binding. In almost all cases, the maximum capacity constraint is only binding for one unique time step in each period. Daily profiles show the constraint is mostly binding between 5am and 7am. Moreover the maximum of these morning peaks necessitate the same heat-pump capacity with daily horizons and with the

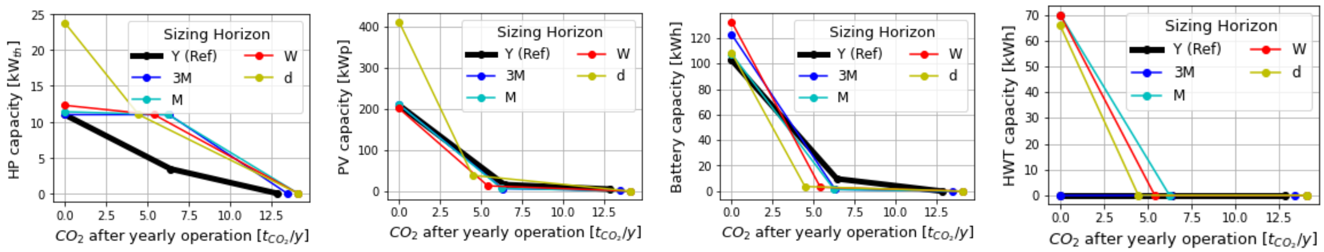

(a) HP in Seattle. (b) PV in Seattle. (c) Battery in Seattle. (d) HWT in Seattle.

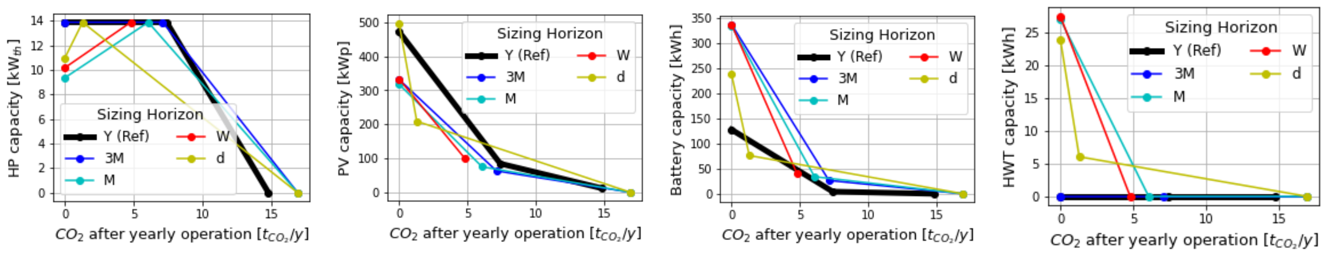

(e) HP in Houston. (f) PV in Houston. (g) Battery in Houston. (h) HWT in Houston.

Figure 3: Renewable capacities optimal front for all carbon emission scenarios for Seattle (3a-3d) and Houston (3e-3h)

Table 2: Ratio of computed cases for which at least one subperiod of the year issued an optimal systems sizing within 5% of reference.

		Duluth			Seattle			Baltimore			LosAngeles			Houston		
		PV	HP	Bat	PV	HP	Bat	PV	HP	Bat	PV	HP	Bat	PV	HP	Bat
Min Cost	3M	.50	.88	.50	.62	1	.50	.50	.88	.50	0	.88	.50	0	.62	.50
	M	.50	.62	.50	.62	.88	.62	.50	.75	.50	0	.75	.50	0	.62	.50
	W	.50	.50	0	.62	.62	.25	.50	.62	0	0	.75	0	0	.62	0
	d	.50	.50	.25	.62	.62	.62	.50	.62	.25	0	.75	.25	0	.62	.25
$-50\%CO_2$	3M	.38	.50	.25	.38	.50	.50	.38	.75	.25	.12	1	.12	0	1	0
	M	.25	.88	.25	.62	1	.12	.12	.75	.38	0	1	.38	.12	1	0
	W	.50	.75	.38	.62	.88	.38	.25	.88	.50	.38	.75	.12	.62	1	0
	d	.62	.88	.62	.75	1	.50	.75	.88	.75	.75	1	.75	1	1	.25
Net Zero	3M	.50	.50	1	1	1	1	1	.50	.50	1	1	1	.50	1	1
	M	.50	0	1	1	.50	1	1	.50	1	0	.50	1	.50	.50	1
	W	1	.50	1	1	.50	1	1	1	1	0	.50	1	.50	.50	1
	d	1	.50	1	1	.50	1	1	1	1	1	.50	1	1	.50	1

yearly reference (red margin in Figure 7).

Figure 7 shows a case where HWT is installed and further highlight the interplay between technologies. Daily profiles show a peak of heat-pump usage at 1pm resulting in an additional need of 7kW$_{th}$ compared to the yearly reference. This 1pm peak comes from the need to rapidly fill the HWT using carbon-free electricity from the PV in winter days.

We also observe a linear relation between the heat-pump capacity designed in the binding constraint and the peak of heating load in that period (Figure 8). Parallel usage of a boiler results in lower heat-pump capacities (e.g. min. Cost and -50% CO_2 in Figure 8), while the use of a thermal storage may lead to higher heat-pump capacities (e.g. NZ in Figure 8) when the thermal storage must be loaded using clean solar power while still ensuring the heating demand (e.g. Daily horizon in Figure 7).

Our observations are different for the battery. Figure 9 shows the constraints related to storage capacities (eq. (3) & (4)) are binding multiple times in each period. The state of charge regularly reaches its maximum (Figure 9a). The ramping constraints are binding almost every day, regardless of the horizon, location, scenario or building type (Figure 9b).

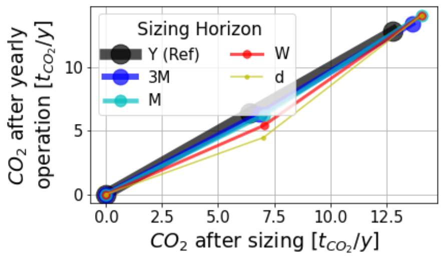

(a) CO_2 emissions in Seattle

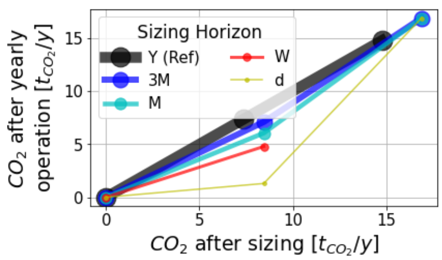

(b) CO_2 emissions in Houston

Figure 4: Carbon emission right after sizing vs. after operation of the so sized system with a yearly horizon.

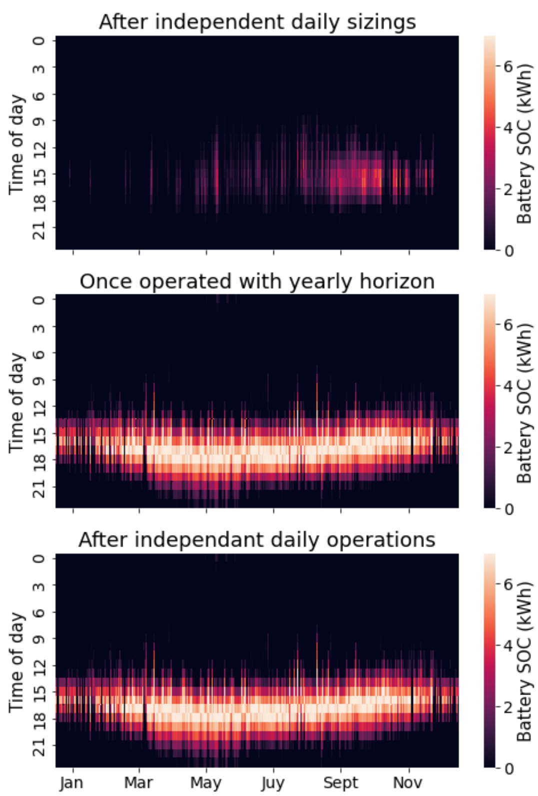

Figure 5: Example of the expected usage of a battery right after the sizing step (top), then after operating the so sized system with horizons of a year (middle) and a day (bottom) in Baltimore (MD).

Therefore storage sizing is found to rely on the entirety of the information, including loads and other decisions taken within the optimization process. Moreover no statistical relation between storage capacity sizing and features from the heating load, the electric load or irradiation was clearly identified.

Computation time

Figure 10 shows computation times required to transform code instructions into solvable problems ("*Create*") and to solve it at both the sizing and operation steps ("*Ope*"). The sizing part shows computational gains as soon as the optimization is performed independently in periods (Figure 10). Computing 52 independent weeks show greater saving in computational resources while 365 days takes up to 60% of the reference time. Adding the operation, the daily horizon shows longest computation times compared to the full time series.

The computation time varies with the building type and systems for small office buildings take more time to compute in the present case. Figure 10 also shows higher computation times for the operation on the full time series, although most of the time is spent to create the problem, while the total solving time is larger for operations in time series subperiods.

Discussion

The same system is sized and operated for different time horizons. To ensure the validity of observations, the experiment is performed in different climate zones, for 2 building types, under different financial and carbon reduction scenarios. Still the procedure is not exhaustive and factors such as the use of simulated loads from archetypes, the use of constant energy prices and efficiencies factors may influence the observations.

Considering the storage looping constraint (eq.1), the methodology suggests a capacity sizing adapted if a specific period (quarter, month, week or day) was repeated indefinitely. A subdivision of the yearly time series holds higher chances to obtain some periods holding accurate results with shorter horizons (Table 2). However shorter horizons also induce higher sensitivity to extreme events, increasing the range of suggested solutions. Therefore risk of oversizing is increased with the current methodology selecting the maximum capacity over all periods. Moreover the yearly cycle and long-term interactions play a dominant role in some cases, and nothing guarantees a-priori the possibility to capture these and obtain accurate sizing using shorter horizons (Figure 6).

The methodology also highlights the importance of storage systems in the decarbonization of building energy demand. Although sizing the battery system inde-

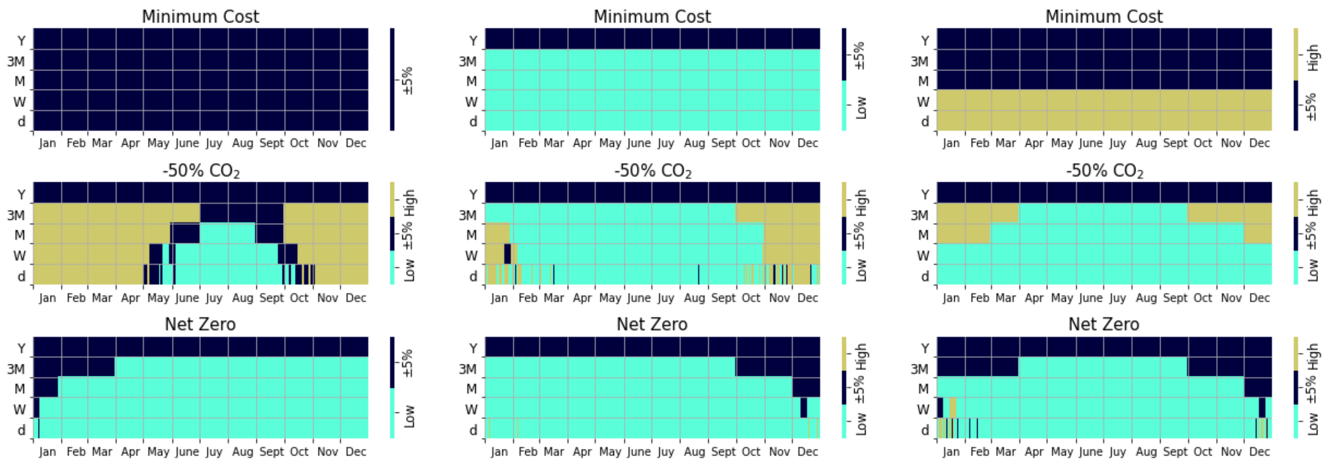

(a) An HP sizing in Los Angeles *(b) A PV sizing in Seattle* *(c) A battery sizing in Baltimore*

Figure 6: Independent periods in which the sizing issues undersized capacities (Low), oversized (High) or similar to the full sizing (± 5%).

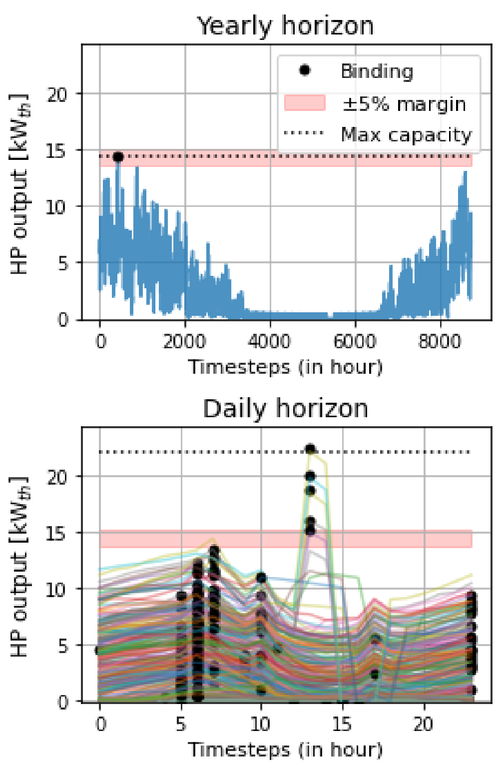

Figure 7: Location of binding constraints for HP capacity sizing in Baltimore for net-zero residential building.

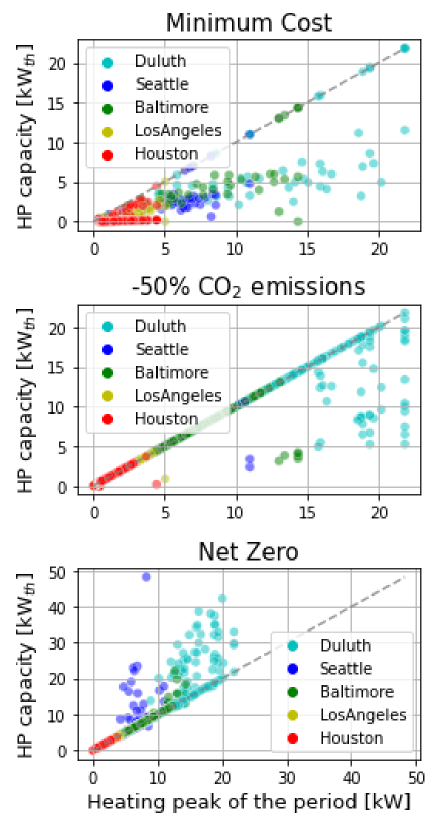

Figure 8: Relation between peak heating load and HP capacity in residential buildings.

pendently in different periods and with different horizons yield a large diversity of suggested capacities, an installed battery is always used at its maximum during the operation step (Figure 5). This contributes in a reduction of expected carbon emissions (Figure 4), as well as a different predicted Heat-Pump and PV production.

Heat storage, mostly suggested for cold places at NZ in our experiment, also perturbs the sizing process, particularly the HP (Table 2). For residential buildings, HWT is designed as additional buffer to absorb peak

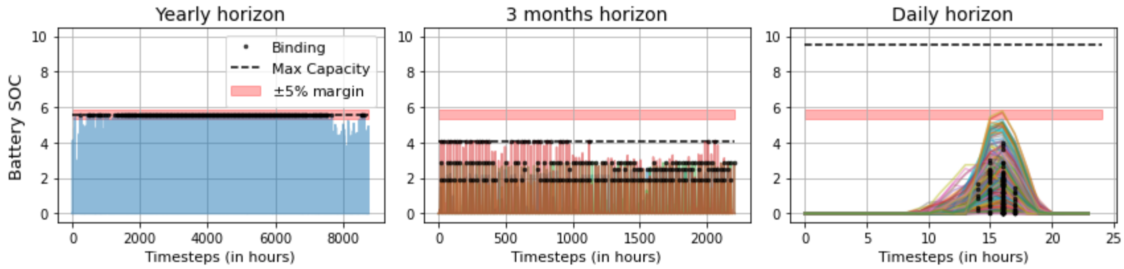

(a) Binding constraints for the storage level of an office building in Los Angeles

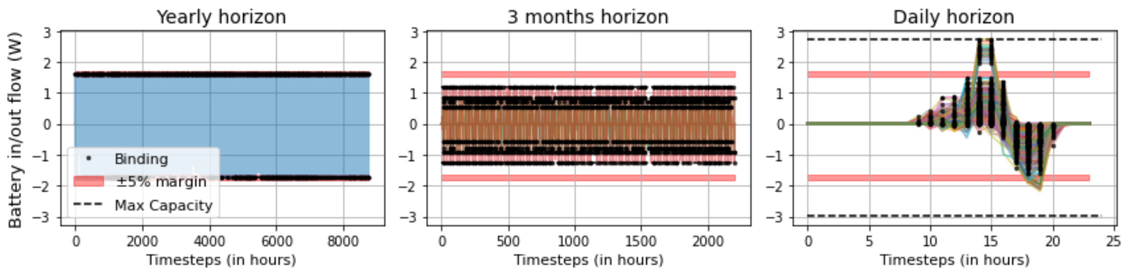

(b) Binding constraints for the storage ramping of an office building in Los Angeles

Figure 9: Decisive moments for the battery sizing: an example in Los Angeles at -50% CO_2 emissions. Both SOC (9a) and in/outflow limits (9b) occur daily. The maximum SOC at a daily horizon matches with the capacity designed with a yearly horizon, though a need to load and discharge faster results to an oversizing.

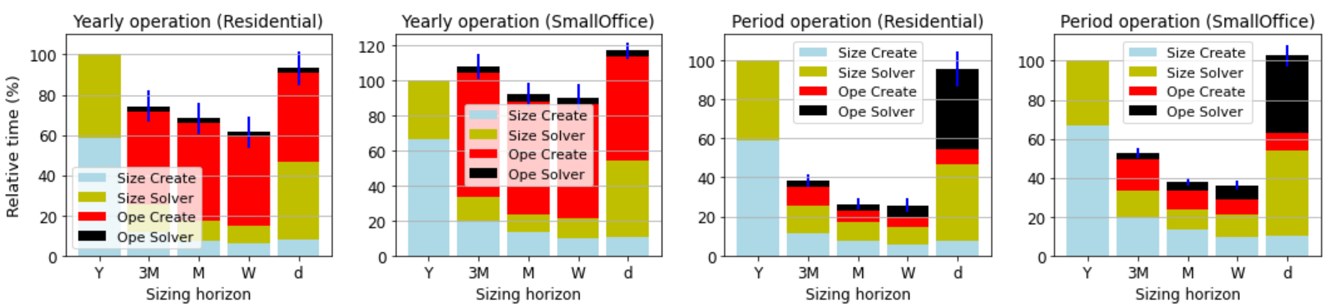

Figure 10: Average relative computation time per building type and operation horizon.

of PV production, forcing the HP to be oversized to produce both to load the storage and meet the heat demand (Figures 7 and 8).

Even during the sizing stage, the storage devices are designed to support the entirety of the system (Figure 9), by being shaped to be used at their maximum at all times. This also influences the sizing of all system components, and highlights the main reason for the present methodology to fail at accurately address an energy hub sizing problem.

On the one hand, the storage system is the difficult piece in models reducing the complexity of energy hub problems (Teichgraeber and Brandt (2022); Kotzur et al. (2021)). On the other hand, the suggested methodology reduces computation time of the sizing step alone. Thus sizing results show a good potential for being used as features in the process of selecting representative days into standard complexity reduction methods.

Conclusion

This study investigates the effect of time horizon on the energy system design via optimization for single buildings. The sizing is performed using portions of the time series data (loads and irradiation) of different length (a day to 3 months).

We found no guarantee that any of the results obtained with shorter horizons are similar to those obtained with a full optimization. Though general trends remain similar. Conversely the system operation is similar regardless of the horizon, once the design and capacities are fixed.

Battery systems drastically influence the sizing results. Storage devices always cycle daily to support the single building loads. At minimum cost or -50% CO_2, both ramping and level of charge are exploited at their maximum on a daily basis, regardless of the considered horizon. At net-zero, the ramping (charging and discharging power) is the decisive element to absorb peaks of solar production.

The interplay of the different technologies in the considered systems does not allow to identify relevant shorter periods to approximate the overall sizing. Thus considering a full year remains necessary to accurately address the sizing. Though the diversity of results obtained with shorter horizons give valuable information on choices made by the solver. Exploiting this information in data-driven processes to select representative periods is of future work's interest.

Acknowledgment

This work used the BESOS platform supported by CANARIE Grant RS-237. (https://besos.uvic.ca)

References

Bahl, B., T. Söhler, M. Hennen, and A. Bardow (2018). Typical Periods for Two-Stage Synthesis by Time-Series Aggregation with Bounded Error in Objective Function. *Front. Energy Res. 5*. Publisher: Frontiers.

Evins, R., K. Orehounig, V. Dorer, and J. Carmeliet (2014, August). New formulations of the 'energy hub' model to address operational constraints. *Energy 73*, 387–398.

Fitiwi, D. Z., F. de Cuadra, L. Olmos, and M. Rivier (2015, October). A new approach of clustering operational states for power network expansion planning problems dealing with RES (renewable energy source) generation operational variability and uncertainty. *Energy 90*, 1360–1376.

Geidl, M., G. Koeppel, P. Favre-Perrod, B. Klöckl, G. Andersson, and K. Fröhlich (2007, April). The energy hub-A powerful concept for future energy systems. In *Third Annual Carnegie Mellon Conference on the Electricity Industry*, Pittsburg, pp. 13–14. Carnegie Mellon.

Gurobi Optimization, L. (2021). *Gurobi Optimizer Reference Manual*.

Hoffmann, M., L. Kotzur, D. Stolten, and M. Robinius (2020). A Review on Time Series Aggregation Methods for Energy System Models. *Energies 13*(3), 1–61. Publisher: MDPI, Open Access Journal.

Kotzur, L., P. Markewitz, M. Robinius, and D. Stolten (2018, March). Impact of different time series aggregation methods on optimal energy system design. *Renewable Energy 117*, 474–487.

Kotzur, L., L. Nolting, M. Hoffmann, T. Groß, A. Smolenko, J. Priesmann, H. Büsing, R. Beer, F. Kullmann, B. Singh, A. Praktiknjo, D. Stolten, and M. Robinius (2021, November). A modeler's guide to handle complexity in energy systems optimization. *Advances in Applied Energy 4*, 100063.

Murray, P., J. Carmeliet, and K. Orehounig (2020, August). Multi-Objective Optimisation of Power-to-Mobility in Decentralised Multi-Energy Systems. *Energy 205*, 117792.

Pfenninger, S. and I. Staffell (2016, November). Long-term patterns of European PV output using 30 years of validated hourly reanalysis and satellite data. *Energy 114*, 1251–1265.

Teichgraeber, H. and A. R. Brandt (2022, April). Time-series aggregation for the optimization of energy systems: Goals, challenges, approaches, and opportunities. *Renewable and Sustainable Energy Reviews 157*, 111984.

Teichgraeber, H., C. P. Lindenmeyer, N. Baumgärtner, L. Kotzur, D. Stolten, M. Robinius, A. Bardow, and A. R. Brandt (2020, October). Extreme events in time series aggregation: A case study for optimal residential energy supply systems. *Applied Energy 275*, 115223.

Westermann, P., T. Christiaanse, W. Beckett, P. Kovacs, and R. Evins (2021, April). besos: Building and Energy Simulation, Optimization and Surrogate Modelling. *JOSS 6*(60), 2677.

Wilson, E. (2014, November). Commercial and Residential Hourly Load Profiles for all TMY3 Locations in the United States.